

## Enhanced efficiency of the dye-sensitized solar cells by excimer laser irradiated carbon nanotube network counter electrode

Yun-San Chien, Po-Yu Yang, I-Che Lee, Chih-Chieh Chu, Chia-Hsin Chou, Huang-Chung Cheng, and Wei-En Fu

Citation: *Applied Physics Letters* **104**, 051114 (2014); doi: 10.1063/1.4864059

View online: <http://dx.doi.org/10.1063/1.4864059>

View Table of Contents: <http://scitation.aip.org/content/aip/journal/apl/104/5?ver=pdfcov>

Published by the [AIP Publishing](#)

---

### Articles you may be interested in

[TiO<sub>2</sub> nanospheres and spiny nanospheres for high conversion efficiency in dye-sensitized solar cells with gel electrolyte](#)

*J. Appl. Phys.* **115**, 134504 (2014); 10.1063/1.4870473

[MgO-hybridized TiO<sub>2</sub> interfacial layers assisting efficiency enhancement of solid-state dye-sensitized solar cells](#)

*Appl. Phys. Lett.* **104**, 063303 (2014); 10.1063/1.4864319

[High performance dye-sensitized solar cell based on hydrothermally deposited multiwall carbon nanotube counter electrode](#)

*Appl. Phys. Lett.* **100**, 243303 (2012); 10.1063/1.4726177

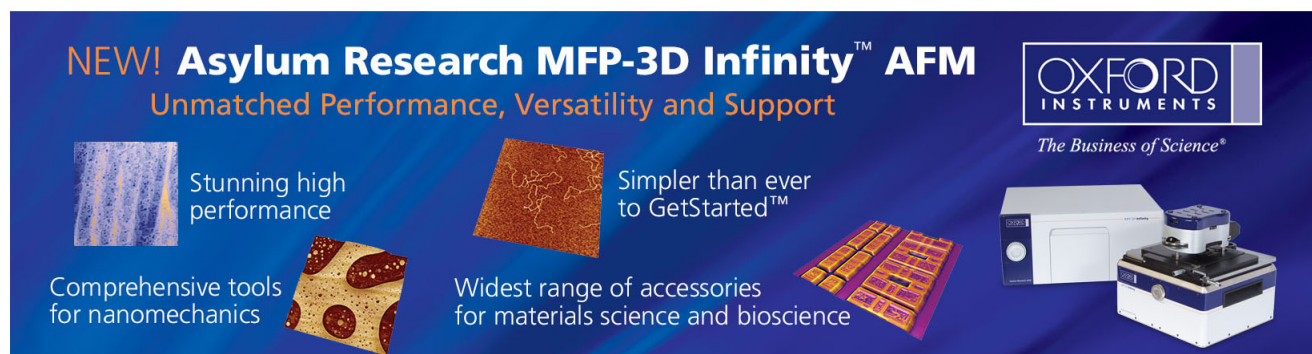
[Laser annealed composite titanium dioxide electrodes for dye-sensitized solar cells on glass and plastics](#)

*Appl. Phys. Lett.* **94**, 071117 (2009); 10.1063/1.3082095

[Platinum/titanium bilayer deposited on polymer film as efficient counter electrodes for plastic dye-sensitized solar cells](#)

*Appl. Phys. Lett.* **90**, 153122 (2007); 10.1063/1.2722565

---

The advertisement features a dark blue background with white and orange text. At the top left, it reads 'NEW! Asylum Research MFP-3D Infinity™ AFM' in large white letters, followed by 'Unmatched Performance, Versatility and Support' in orange. On the right, the Oxford Instruments logo is shown with the tagline 'The Business of Science®'. Below the text are several images: a blue textured surface, a brown textured surface, a grid of small square samples, and the MFP-3D Infinity AFM instrument itself. Text boxes describe the instrument's capabilities: 'Stunning high performance', 'Simpler than ever to GetStarted™', 'Comprehensive tools for nanomechanics', and 'Widest range of accessories for materials science and bioscience'.

## Enhanced efficiency of the dye-sensitized solar cells by excimer laser irradiated carbon nanotube network counter electrode

Yun-San Chien,<sup>1,(a)</sup> Po-Yu Yang,<sup>2</sup> I-Che Lee,<sup>3</sup> Chih-Chieh Chu,<sup>3</sup> Chia-Hsin Chou,<sup>3</sup> Huang-Chung Cheng,<sup>3</sup> and Wei-En Fu<sup>1</sup>

<sup>1</sup>Center for Measurement Standards, Industrial Technology Research Institute, Hsinchu, Taiwan

<sup>2</sup>Taiwan Semiconductor Manufacturing Company, Hsinchu, Taiwan

<sup>3</sup>Department of Electronics Engineering and Institute of Electronics, National Chiao Tung University, Hsinchu, Taiwan

(Received 24 September 2013; accepted 18 January 2014; published online 4 February 2014)

The carbon nanotube network decorated with Pt nanoparticles (PtCNT) irradiated by excimer laser as counter electrode (CE) of dye-sensitized solar cells (DSSCs) has been systematically demonstrated. The conversion efficiency would be improved from 7.12% to 9.28% with respect to conventional Pt-film one. It was attributed to the enhanced catalytic surface from Pt nanoparticles and the improved conductivity due to the adjoining phenomenon of PtCNTs irradiated by laser. Moreover, the laser annealing could also promote the interface contact between CE and conductive glass. Therefore, such a simple laser-irradiated PtCNT network is promising for the future flexible DSSCs applications. © 2014 AIP Publishing LLC. [<http://dx.doi.org/10.1063/1.4864059>]

Solar cell has been attracted much attentions owing to its potential as the future reusable energy source. As compared to the silicon-based solar cells, dye-sensitized solar cells (DSSCs) fabricated by Grätzel and O'rgan in 1991 possessed the lower device cost and flexible structures which were suitable for the future portable and transparent energy supply.<sup>1</sup> The Pt film was extensively utilized as the counter electrode (CE) of the DSSCs for its good electrical conductivity, chemical stability, and high electrocatalytic properties with electrolyte.<sup>2,3</sup> However, the high cost and corrosion in the electrolyte of Pt film increased the demand of new materials as the CEs. Therefore, there were many substitutes for CEs such as graphene layers, CNTs, and conductive polymer composites. Among these, the graphene and CNTs with high surface-to-volume ratio, excellent mechanical and electrical properties, and chemical stability had widely demonstrated the promising properties. To obtain the comparable characteristics with the Pt CEs, the Pt nanoparticles supported by CNTs (PtCNT) network had already been demonstrated to exhibit the improved photoelectrical properties. Although, the usage of the noble Pt metals could be significantly reduced, the micrometer thickness for the PtCNT CEs was derived to obtain the equal performance with Pt ones, and<sup>4,5</sup> such a thick PtCNT CE would increase the material usage and remain opaque. Therefore, the additional post treatment was needed to further improve the performance of DSSCs. In this Letter, the excimer laser was therefore utilized to modify the PtCNT structure into the hybrid graphene sheet (GS) and CNT structures decorated by Pt nanoparticles. Such a semi-transparent PtCNT CE could remarkably improve the conversion efficiency with 30% as compared with the conventional Pt CE.

The CNTs were oxidized by H<sub>2</sub>SO<sub>4</sub>/HNO<sub>3</sub> solution. Then, the oxidized CNTs were mixed with chloroplatinic acid (H<sub>2</sub>PtCl<sub>6</sub>) in ethylene glycol solution at 140 °C for 1 h.

Subsequently, the obtained homogeneous PtCNT solution was ultrasonically sprayed on the fluorinated tin oxide (FTO) conductive glass. A PtCNT continuous network with the thickness of approximately 700 nm was formed via the multiple spraying. Then, the PtCNT network was placed into a chamber pumped down to  $2 \times 10^{-2}$  Torr and irradiated using the KrF excimer laser ( $\lambda = 248$  nm) with the laser energy densities ranged from 100 to 700 mJ/cm<sup>2</sup>. The laser energy operation started from 100 mJ/cm<sup>2</sup> increased to 600 mJ/cm<sup>2</sup> with the each elevated energy difference of 100 mJ/cm<sup>2</sup> under the 98% overlapping ratio (i.e., 50 shots) for the CE usage. The TiO<sub>2</sub> active layers with the diameters of 20 nm and 200 nm were coated on the FTO substrate by the repeated doctor blade method, respectively, followed by 500 °C thermal annealing. Such a working electrode (cell area: 0.5 cm × 0.5 cm) was immersed into the 1 mM N719 dye solution in acetonitrile and *tert*-butanol (TBP) for 24 h. The working electrode and the counter one were assembled with the polyimide spacer. The electrolyte (0.1 M LiI, 0.1 M PMII, 0.05 M I<sub>2</sub>, and 0.5 M TBP in the MPN solution) was injected into the assembled cell. The current-voltage measurement (Keithley 2400) was operated under the 1.5 AM solar simulator (Oriel) with the light intensity fixed at 100 mW/cm<sup>2</sup>. The electrochemical impedance spectroscopy (EIS) was measured by a potentiostat (EG&G 273 a) equipped with a frequency response analyzer (EG&G 1025); AC signal with 10 mV amplitude was applied with a recorded frequency that ranged from 10<sup>5</sup> to 10<sup>-2</sup> s<sup>-1</sup>. The fitting of the impedance spectroscopy was implemented by Zview software.

Fig. 1(a) displays the SEM micrograph of the top view of as-sprayed PtCNT network with uniform surface morphology. The structures of CNTs remained the tube shape without deterioration by the strong oxidant. Fig. 1(b) demonstrates the TEM pictures which display the uniform distributed Pt nanoparticles with the size of 2–3 nm. The HRTEM image of PtCNTs in the inset of Fig. 1(b) shows the well-dispersed Pt nanoparticles over the CNT sidewalls.

<sup>a)</sup>Author to whom correspondence should be addressed. Electronic mail: u930347@oz.nthu.edu.tw.

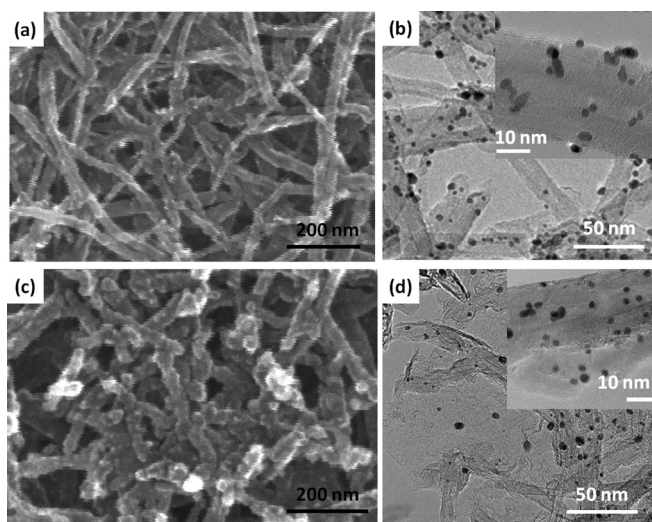


FIG. 1. (a) The SEM image and (b) the TEM image of the as-sprayed PtCNT network. The inset shows the HRTEM of PtCNT. (c) The SEM image and (d) the TEM image of the laser-irradiated PtCNT ( $600 \text{ mJ/cm}^2$ ) network, and the inset displays the HRTEM of exfoliated PtCNT after laser irradiation.

It depicted that the solution process decorating Pt nanoparticles facilitated the smaller and uniform size distribution. The SEM image of the laser-irradiated PtCNT network is illustrated in Fig. 1(c). As compared with the as-sprayed network, the surface morphology with the enlarged tube diameters observed flatter and thin-film-like. The surface roughness measured by atomic force microscopy (AFM) decreased from  $35.78 \text{ nm}$  to  $14.24 \text{ nm}$  after laser irradiation. Fig. 1(d) demonstrates the HRTEM images of the laser-irradiated PtCNT network. According to the previous literatures,<sup>6,7</sup> the CNTs would be unzipped by high laser energy along the longitudinal direction into the fully exfoliated GS. Consequently, some of the CNTs appeared to be unzipped as the film structures, and the hybrid structures of CNTs and GS were formed after laser irradiation of the PtCNT

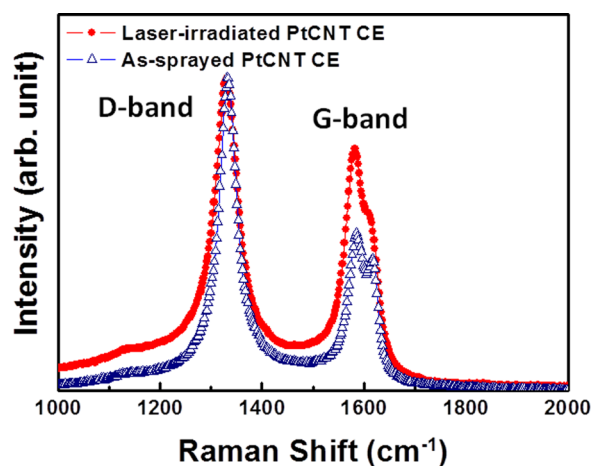


FIG. 2. The Raman spectrum of the as-sprayed and laser-irradiated PtCNT network ( $600 \text{ mJ/cm}^2$ ).

network. Furthermore, the Pt nanoparticles were also found to be well dispersed on such a hybrid structure, which is similar to the ones without laser irradiation, as displayed in the inset of Fig. 1(d). The well-dispersed Pt nanoparticles demonstrated the remained high catalytic reacting surface after laser irradiation.

The Raman spectrum demonstrates the crystallinity variations after the laser irradiation, as illustrated in Fig. 2. There are two peaks, G-peak and D-peak, can be observed. The G-peak ( $1584 \text{ cm}^{-1}$ ) was assigned to the  $\text{sp}^2$ -bonding of CNTs, while the D-peak ( $1322 \text{ cm}^{-1}$ ) was ascribed to the existence of crystal defects, amorphous carbon, and dangling bonds.<sup>8</sup> After the excimer laser irradiation, the  $I_{\text{D}}/I_{\text{G}}$  ratios were obviously decreased from 1.98 to 1.11. In addition, the  $\text{D}'$  band ( $1610 \text{ cm}^{-1}$ ) was also assigned to the existence of crystal defects. Similarly, the reduced  $\text{D}'$  band intensity also proved the better crystallinity after laser irradiation.<sup>9</sup>

The schematic diagram of the fabricated DSSC with the PtCNT network as the CE is shown in Fig. 3(a). The variations of the conversion efficiency and the sheet resistance

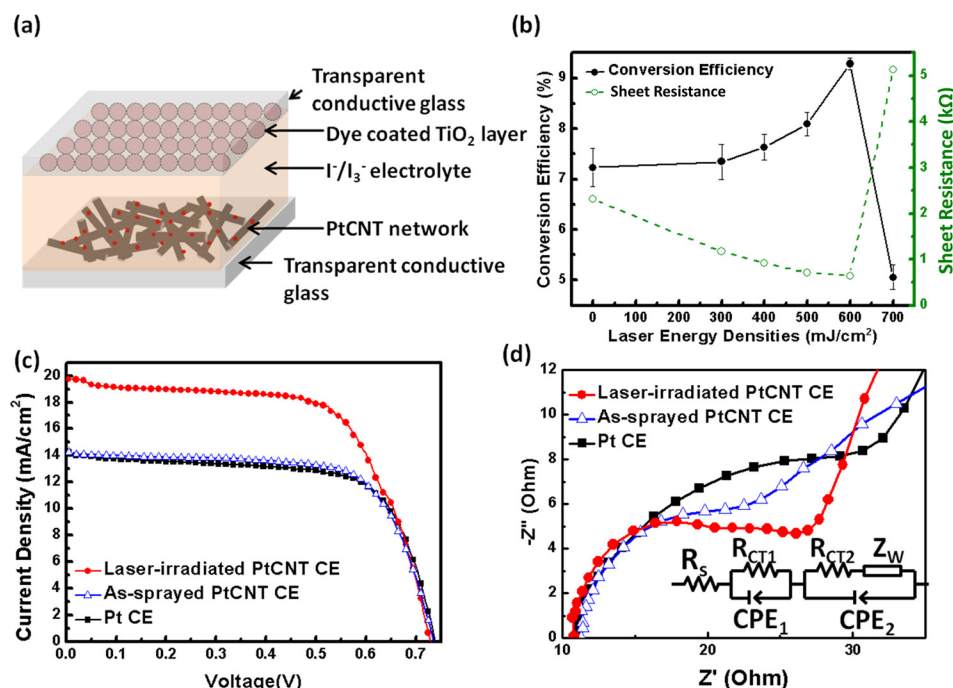


FIG. 3. (a) The fabricated DSSCs with the PtCNT network as CE. (b) The conversion efficiency and sheet resistance versus the applied excimer laser energy densities. (c) The  $J$ - $V$  characteristics of the DSSCs with Pt, as-sprayed PtCNT, and laser-irradiated PtCNT ( $600 \text{ mJ/cm}^2$ ) network. (d) The Nyquist plot measured at open-circuit condition.

TABLE I. The  $J$ - $V$  characteristics of DSSCs using the Pt, as-sprayed PtCNT, and laser-irradiated PtCNT (600 mJ/cm<sup>2</sup>) network as the CEs.

Counter electrode	$J_{sc}$ (mA/cm <sup>2</sup> )	$V_{oc}$ (V)	FF	Efficiency (%)
Pt	14.19	0.74	0.68	7.12
As sprayed PtCNT	14.26	0.74	0.69	7.23
Laser-irradiated PtCNT	19.73	0.74	0.66	9.28

with the laser energy densities are illustrated in Fig. 3(b). With the elevating the applied laser energy, the GS began to appear to form a continuous conductive paths. In addition, the crystallinity was also remarkable enhanced under the laser treatment. Therefore, the efficiency would begin to be improved obviously, owing to the surface morphology modification occurrence. As the laser energy reached 600 mJ/cm<sup>2</sup>, the optimized efficiency could attain 9.28%. However, the efficiency was dramatically reduced to 5.056% as the laser energy was increased to 700 mJ/cm<sup>2</sup>. The efficiency reduction was resulted from the ablation of PtCNT network occurrence, causing the interrupted conducting paths and decreased charge transferring ability. In addition, the transparency of PtCNT network was proportional to the laser energy, implying the GS production. The cleaved GS from CNTs would reduce the light passing carbon layers, hence that would increase the transmittance as the laser energy elevated. The photocurrent-voltage ( $J$ - $V$ ) characteristics of DSSCs with the conventional Pt film, the as-sprayed PtCNT network, and the laser-irradiated PtCNT (600 mJ/cm<sup>2</sup>) one as the CEs are displayed in Fig. 3(c). The cell parameters of various CEs are summarized in Table I. The results indicate that the short-circuit current  $J_{sc}$  increased from 14.19 to 14.26 mA/cm<sup>2</sup>, and the conversion efficiency improved from 7.12% to 7.23% after the Pt electrode was replaced as the as-sprayed PtCNT one. The improved electrical characteristics were ascribed to the three-dimensional structures of PtCNT network. Furthermore, after the excimer laser irradiation, the  $J_{sc}$  could be significantly promoted to 19.73 mA/cm<sup>2</sup> and the efficiency to 9.28%, as compared with the as-sprayed PtCNT CE. The remarkably enhanced  $J_{sc}$  was ascribed to the better charge transferring ability and interface impedance.<sup>10,11</sup> This around 30% enhancement was ascribed to the GSs occurrence. The exfoliated CNTs to form GSs extended the conducting paths and contacting area with electrolyte. For the as-sprayed PtCNT network, the electrical transporting merely relied on discrete contact junctions, therefore exhibiting deteriorated properties. The exfoliated CNT layers after excimer laser irradiation expanded the conducting paths and contact area with electrolyte, hence improving the electrical characteristics and redox ability. In addition, for the laser-irradiated PtCNT network, the series resistance was fitted to decrease from 6  $\Omega$  cm<sup>2</sup> to 5.65  $\Omega$  cm<sup>2</sup> as compared to the conventional Pt one, demonstrating the improved charge transferring ability of laser-irradiated one.<sup>12</sup>

For further confirming the laser-irradiation effects on the photovoltaic properties, the EIS measurement was conducted to evaluate the charge-transfer resistance ( $R_{CT}$ ). Fig. 3(d) illustrates the Nyquist plot of the Pt, as-sprayed

PtCNT, and laser-irradiated PtCNT thin film as the CEs measured at open-circuit condition. The first semicircle represents the contact resistance between the electrolyte and CE. According to the radius of first frequency semicircle, the  $R_{CT}$  of Pt and as-sprayed PtCNT CEs were fitted to be 28.24  $\Omega$  and 25.72  $\Omega$ . In contrast, the  $R_{CT}$  was notably reduced to 19.12  $\Omega$  after the laser irradiation. There were three possible reasons for the reduction impedance of the laser-irradiated PtCNT CE. First, the excimer laser irradiation would produce the instantaneous heat to melt the FTO and merge with CNT network. Therefore, the electrical contact between the transparent conducting film and CE was improved. The contact improvement via thermal annealing was already proven to be capable of promoting the increased efficiency.<sup>13</sup> Second, the excimer laser irradiation exfoliated the CNTs into GS layers stacking. The expanded GS layers could act as conductive paths and improve the overall network electrical characteristics. Finally, the exfoliated GS layers could not only increase the contact surface area with electrolyte, but also sustain the original three-dimensional structures for the electrolyte to diffuse and react. As compared with the conventional Pt and as-sprayed PtCNT CEs, the superior electrical characteristics for the laser-irradiated PtCNT DSSCs were attributed to the modified surface morphology and the further improved electrical contact.

The excimer laser irradiation has been performed on the PtCNT network as the CE of the DSSCs to achieve a high short-circuit current of 19.73 mA/cm<sup>2</sup> and superior conversion efficiency of 9.28%, respectively. As compared with the Pt film as CE, the as-sprayed PtCNT network could attain the improved characteristics ascribing the three-dimensional catalytic surface area. Furthermore, with the excimer laser irradiation, part of the CNTs would be unzipped into GS layers, resulting in the GS and CNTs hybrid structures. The promoted conversion efficiency is attributed to the cleaved structures to elevate the electrical conductivity and the reactive surface area with electrolyte. Moreover, the instantaneous heat of the irradiated laser beam assists the merged structures with FTO. Therefore, the semi-transparent laser-irradiated PtCNT network is promising for the future applications in flexible DSSCs.

The authors thank the National Science Council of the Republic of China for their support under Contract No. 101-2221-E-009-077-MY3. Also thanks to the Nano Facility Center (NFC) in National Chiao Tung University and the National Nano Device Laboratory (NDL) for technical supports.

<sup>1</sup>B. O'regan and M. Grätzel, *Nature* **353**, 737 (1991).

<sup>2</sup>Y. Chiba, A. Islam, Y. Watanabe, R. Komiya, N. Koide, and L. Han, *Jpn. J. Appl. Phys., Part 2* **45**, L638 (2006).

<sup>3</sup>M. Grätzel, *Inorg. Chem.* **44**, 6841 (2005).

<sup>4</sup>T. N. Murakami, S. Ito, Q. Wang, Md. K. Nazeeruddin, T. Bessho, I. Cesar, P. Liska, R. Humphry-Baker, P. Comte, P. Péchy, and M. Grätzel, *J. Electrochem. Soc.* **153**, A2255 (2006).

<sup>5</sup>W. J. Lee, D. Y. Lee, I. S. Kim, S. J. Jeong, and J. S. Song, *Trans. Electr. Electron. Mater.* **6**, 140 (2005).

<sup>6</sup>Y. S. Chien, W. L. Tsai, I. C. Lee, J. C. Chou, and H. C. Cheng, *IEEE Electron Device Lett.* **33**, 1622 (2012).

- <sup>7</sup>P. Kumar, L. S. Panchakarla, and C. N. R. Rao, *Nanoscale* **3**, 2127 (2011).
- <sup>8</sup>P. C. Eklund, J. M. Holden, and R. A. Jishi, *Carbon* **33**, 959 (1995).
- <sup>9</sup>Y. S. Chien, I. C. Lee, P. Y. Yang, C. L. Wang, W. L. Tsai, K. Y. Wang, C. H. Chou, and H. C. Cheng, *Appl. Phys. Lett.* **102**, 183111 (2013).
- <sup>10</sup>H. Zhu, H. Zeng, V. Subramanian, C. Masarapu, K. H. Hung, and B. Wei, *Nanotechnology* **19**, 465204 (2008).
- <sup>11</sup>K. M. Lee, C. W. Hu, H. W. Chen, and K. C. Ho, *Sol. Energy Mater. Sol. Cells* **92**, 1628 (2008).
- <sup>12</sup>W. Q. Liu, L. H. Hu, S. Y. Dai, L. Guo, N. Q. Jiang, and D. X. Kou, *Electrochim. Acta.* **55**, 2338 (2010).
- <sup>13</sup>S. Siriroj, S. Pimanpang, M. Towannang, W. Maiaugree, S. Phumying, W. Jareamboon, and V. Amornkitbamrung, *Appl. Phys. Lett.* **100**, 243303 (2012).